Health Biotechnology and Biopharma (2023), 6(4): 25-42

Original Research Article

Experimental studies and artificial neural networks (ANN) modeling of asparaginase partitioning in aqueous two-phase systems: Polyethylene glycol and inorganic salts

Mohsen Mesbahi-Nowrouzi[1], Soroush Sardari[1,*]

[1]Drug Design and Bioinformatics Unit, Medical Biotechnology Department, Biotechnology Research Centre, Pasteur Institute of Iran, Tehran, Iran

***Corresponding author:** Soroush Sardari, Drug Design and Bioinformatics Unit, Medical Biotechnology Department, Biotechnology Research Centre, Pasteur Institute of Iran, Tehran, Iran. E- mail: sardari@pasteur.ac.ir*

DOI: 10.22034/HBB.2023.03

Received: October 8, 2022; **Accepted:** October 26, 2022

ABSTRACT

This article studied applicabilities of Artificial Neural Networks (ANN), aiming at partitioning of Asparaginase (ASP). The first step investigated the partitioning of ASP using ATPS, consisting of polyethylene glycol and different inorganic salts. The studies of ASP partition were conducted by measuring the amounts of ASP in the upper and lower phase, followed by calculating the recovery. PEG of 6000 and (NH4)2SO4 provided the best performance with recovery yield of 86 %. The partitioning behavior of the approach was investigated in the presence of an impurity kind of amylase. Related partition coefficient of 0.21 and recovery yield of ASP of 86 % were calculated. A Circular Dichroism (CD) spectroscopy compared the structure of standard and partitioned ASP, which remained stable. The relative activity was determined to be 94 %. A feed-forward neural network was applied to predict the best model to partition of ASP.

***Keywords*:** Asparaginase; ATPS; artificial neural networks

INTRODUCTION

Nowadays, aging population and deficiency of traditional drugs increase the demand for new therapies such as biopharmaceutical products [1]. Biotechnology develops the upstream processing and improves their productions from various sources in higher yields. Nevertheless, the downstream processes are neglected because of less tendency of biopharmaceutical companies to replace

common processes with new strategies. The limit for this replacement is that these manufactures should allocate 80 % of the total manufacturing cost to downstream processing. Now chromatography method is mainly practical in this step. However, it has restrictions such as complexity, operating, low capability in process integration, laborious processing cycles, economical aspects and environmental matters [2-4]. The researchers put significant efforts to present new non-chromatography strategies to develop the process throughput and decrease the processing time. Liquid–liquid extraction [5], membrane separation [6], high performance tangential flow filtration [7], affinity precipitation [8], high gradient magnetic fishing [9] and crystallization [10] are some common examples of these methods. Aqueous two-phase system is another qualified candidate in extraction, separation, purification, and enrichment of biomolecules [11]. These systems are formed by mixing two immiscible components for example two immiscible, above their critical concentrations [12,13]. ATPSs are easy to be operated, reliable, environmentally biocompatible, energy efficient and inexpensive. Moreover, it is one-step process and steps of clarification, concentration and purification can be integrated [14].

Up to now, different analytes were separated by this method. For example, a carbohydrate-based aqueous two-phase system separated and purified glatiramer acetate and amino acids [15]. Also, a mixture of PEG and DEX was used to remove soluble aggregates of IgG by ATPS [16]. In another research, Azevedo presented ATPS of PEG and dextran for the integrated purification of the anti-CD34 mAb [17]. Additionally, 15 proteins were partitioned in PEG–sodium sulfate ATPS successfully [18].

In this article, ATPSs, consisting of PEGs and inorganic salts, were applied to partition Asparaginase (ASP). ASP is a FDA-approved biopharmaceutical for Acute Lymphoblastic Leukemia (ALL). The phase diagrams such as binodal and tie-lines were determined, the effective parameters with respect to the kinds of polyethylene glycol, inorganic salts and pH were screened; afterwards, the partition coefficients and recoveries were reported. The partitioning of secondary protein (amylase) as an impurity was investigated. Structure and activity of ASP were analyzed and compared before and after partitioning with a standard sample. A

weakness of ATPSs application is their complexity so the partitioning mechanism is hard to be understood. In reference to, they are based on trial-and-error screening approaches. Artificial Neural Network (ANN) is an efficient approach to overcome this challenge, which models the partitioning ASP in ATPS in this study.

MATERIALS AND METHODS

$Na_3C_6H_5O_7$. $2H_2O$, NaH_2PO_4, K_2HPO_4, $(NH_4)_2SO_4$, PEG (Mw: 4000, 6000 and 10000), L-Asparagine, Nessler′s reagent were purchased from Merck (Merck, Germany) in the analytical grade. The analytical grade of ASP, amylase and Trichloroacetic Acid (TCA) were prepared from Sigma-Aldrich. The double-distilled water is used in all experiments.

Phase diagram determination

The determination of phase diagram for the systems was conducted at room temperature (25 ± 1 °C) and atmospheric pressure by using the cloud-point method [19]. The system was prepared via adding exact amounts of salt solution to the polymer solution. At a critical point (the could-point), the mixture turn to a turbid sample and a two-phase system was achieved. The mixture composition was recorded, followed by providing a point on the binodal curve. Then, through adding distilled water drop by drop to the tube, a clear one-phase system was achieved and adding more salt solution turn it to a two-phase system. Merchuk's equation (Eq. 1) was applied to fit the binodal curve [20].

$$[Y] = A \times \exp\{(B \times [X]^{0.5}) - (C \times [X]^3)\} \quad (1)$$

Where [Y] and [X] stand for polymer and salt weight percentages in binodal curves. The constants of A, B and C are found by regression of the experimental data. The components of each phase and the related tie-lines (TLs) were calculated using the lever-arm rule regarding Eq. (2) – (5) [21]:

$$[Y]_T = A \times \exp\{(B \times [X]_T^{0.5}) - (C \times [X]_T^3)\} \quad (2)$$

$$[Y]_B = A \times \exp\{(B \times [X]_B^{0.5}) - (C \times [X]_B^3)\} \quad (3)$$

$$[X]_T = (\frac{[Y]_M}{m}) - (\frac{1-m}{m}) \times [Y]_B \quad (4)$$

$$[X]_T = (\frac{[X]_M}{m}) - (\frac{1-m}{m}) \times [X]_B \quad (5)$$

In the equations of 2 to 5, M, T and B define the mixture point, top and bottom phase, respectively; m defines as following:

$$m = \frac{M_{top}}{M_{total}} \quad (6)$$

Eq. 7 determines the tie-line lengths (TLLs).

$$TLL = \sqrt{([X]_T - [X]_B)^2 + ([Y]_T - [Y]_B)^2}$$

(7)

Preparation of ATPS

ATPS composition was mixed together according to the obtained binodal diagram. ATPS (10 g) was prepared through mixing exact quantities of solid chemicals (PEG and inorganic salts), ASP solution (2 mg mL^{-1}) and distilled water, followed by being shaken for one hour. Phase separation was done by centrifuging the samples at 3,500 rpm for 40 minutes at room temperature. A glass Pasteur pipette separated the upper and lower phases. The total concentration of protein was analyzed and partition coefficient (KAsp) and recovery yield (YT) parameters were calculated. Partition coefficient (KAsp) describes the protein ratio in the upper phase to the lower phase.

$$K_p = \frac{[ASP]_T}{[ASP]_B}$$

(8)

Where [ASP]T and [ASP]B are the ASP amounts in the upper and lower phases, respectively [22].

Y_T is calculated at the phase containing the more concentration of target analyte. It contributes to the initial ASP amount in the sample, loaded to the ATPS.

$$Y_T = \frac{[ASP]_t \times V_t}{[ASP]_i \times V_i}$$

(9)

In this equation, $[ASP]_t$ and V_t are ASP concentration and volume of the phase containing more concentration of ASP, respectively. $[Asp]_i$ expresses the concentration and V_i is the volume of the stock solution added to the system [23].

Analytical techniques section

Protein assay

The concentrations of protein were evaluated with Bradford approach that ASP was as the standard [24].

UV Circular Dichroism (CD) spectroscopy

The analysis started by adding $(NH_4)_2SO_4$ to the sample of ASP to increased its concentration and then centrifuged at 5000 rpm for 20 min and temperature of 25 ± 1 ° C. Afterwards, the supernatant was thrown and the residual solution was added to a centrifugal filter unit with a 50 kDa molecular weight cut-off. The solution was centrifuged at 5000 rpm for 40 minutes at room temperature. The ASP structure was followed by a far UV CD spectroscopy (Jasco, J-810; Japan). The protein concentration was 0.5 mg mL^{-1}.

J700 CD-JASCO software calculated the secondary structure parameters. Since ellipticity values depend on the ASP

concentration, a same concentration of ASP was applied as treated and untreated samples, regarding Bradford method. Each experiment was conducted in triplicate and the related mean values were considered for comparison.

ASP activity assay

Wriston and Yellin's method determines ASP activity, using nesslerization to measure the released ammonia concentration [25]. The sample (2 mL) containing of ASP (1.5 mL, 0.04 M), enzyme (0.5 mL) and Tris-HCl buffer (0.05 M, pH 8.6) was prepared, followed by being incubated at 37 °C for 30 min. TCA (0.5ml, 1.5 M) ended the reaction.

The precipitated protein was removed by a centrifuge (5 min) and the top solution (0.5 ml) and distilled water (7 ml) was collected to quantify the released ammonia by adding Nessler's reagent (1 ml). After 20 min, yellow color of mixture represents ammonia, which was measured by a UV-Visible spectrophotometer at the absorbance of 480 nm (Bio-Rad Laboratories, SmartSpec Plus, USA). The amount of released ammonia from the test sample was carried out by comparing the absorbance of solutions of NH_4Cl as the reference. One Unit (U) of ASP is the amount of enzyme, which released one μmole of ammonia at 37 °C at pH of 8.6 in one min. The activity ratio of treated ASP and untreated ASP was reported as relative activity.

ANN modeling

The 'nntool' in MATLAB toolbox (MATLAB R2020b, MathWorks, Natick, Mass., USA) analyzed the data in ANN model. The backpropagation *a*lgorithm performs learning on a two-layer feed-forward neural *network*. In this technique, a feed-forward algorithm was applied in order to investigate the output, along with backpropagation, related to the weights recursively. The Levenberg–Marquardt backpropagation Algorithm (LMA) was the best fitted algorithm to train the network (input: 15 parameters and output: one output (K_{ASP})). Different networks with different numbers of hidden neurons were used and a one-hidden layer model was selected because it was effective on modeling the K_{ASP} of ASP in ATPS. The network optimization, such as optimum numbers of neurons in the hidden layer, plays important part in ANN modeling. Accordingly, different numbers, ranging from one to 10 were selected and the input and output variables were randomly divided to 70% for training and 15% for network validation. The remain 15 % was

used for completely independent test of network generalization. Hyperbolic tangent sigmoid transfer function is used for the hidden and the output layers. During the learning process, the estimated output and the target were compared together, also the system error generates a model with a particular weight to express the selected system property.

Evaluation of the models was completed by comparison the model accuracy, separately for (i) training, (ii) validation, (iii) testing, and (iv) overall model, according to correlation coefficient (R), determination coefficient (R^2) and mean squared error (MSE) (Eq. 11 – 13).

$$MSE = \frac{1}{N}\sum_{i=1}^{N}(t_i - y_t)^2 \quad (11)$$

$$MSE = \frac{100}{N}\sum_{i=1}^{N}\left|\frac{t_i - y_i}{t_i}\right| \quad (12)$$

$$R^2 = \frac{\sum_{i=1}^{N}(t_i - t_m^2 - \sum_{i=1}^{N}(t_i - y_i)^2)}{\sum_{i=1}^{N}(t_i - y_i)^2} \quad (13)$$

In these equations, N, t and y are the number of data points, the target (experimental) data, and the anticipated value, respectively.

RESULTS

Phase diagrams: Binodal curves and tie-lines

Data on binodal curves of ATPSs under study shows areas where phase separation and consequently extraction could be happened. The binodal curves of ATPSs were plotted, eight tie lines were drawn and final compositions including salts, PEG and water were achieved by linear regression fitting (Figure 1 a-l). The constants and the correlation coefficients (R^2) are calculated based on the mentioned equations 1-7 (Table 1).

Preliminary studies on the partition behaviour of ASP

In this study, the partition coefficients of ASP in an ATPS were determined. The maximum recovery (96 %) of ASP was obtained in the bottom phase consisting of PEG 4000 (15 %) and $Na_3C_6H_5O_7$. $2H_2O$ (25 %) at the pH of 6.8. The concentrations of PEG and salt impact on the ATPS recovery yield. However, the recovery of 88 %, which is related to sample of PEG 10000 (25 %) and K_2HPO_4 (16 %) shows a promising result.

The optimal separation conditions

The selectivity of the ASP separation procedure was investigated in the presence of an impurity kind of amylase (one mM)

and the feed (10 g). Table 2 summarizes the reports. In S1, K_p amount is close to one (0.98), confirming same concentration of ASP in both phases and not being partitioned. This system is not recommended. The amounts of Kp increased in systems S2 and S3, which show efficient ASP separation because ASP and amylase were partitioned in two different phases. S2 and S3 were selected for further experiments by CD.

CD Spectroscopy & Steady-state kinetic study

CD results of S2 were not satisfying; however, ASP in S3 was isolated from the bottom phase of the optimized feed, showing no significant alterations in the amounts of secondary structures compared to the ASP standard solution (0.5 mg mL^{-1}). The results of S2 and S3 are provided

Figure. 2 (a – d). The secondary structure estimation of standard ASP showed α-Helix (23.5 %), β-Sheet (14.1 %), β -Turn (29.4 %) and random structure (33.1 %). These structures in S2 were characterizes as 19.5 %, 33.7 %, 18.1 % and 28.7 % for the structures of α-Helix, β-Sheet, β -Turn and random structure, respectively. But, the estimation of the secondary structure of isolated ASP from the optimum feed illustrates 24.6 % of α-Helix, 18.4 % of β-Sheet, 23.4 % of β -Turn and 33.6 % of random structure. The standard and the optimum feed, in Figure 2, shows a minimum peak at 216 nm, attributing to the α-helix secondary structure, no significant differences were observed.

Table 1 Merchuk's parameters and R^2 obtained by fitting Eq. 1

Salt	Polymer	A	B	10^5C	R^2
$Na_3C_6H_5O_7$, $2H_2O$	PEG 4000	60.1950	-0.3493	47.90513	0.995
	PEG 6000	57.2989	-0.3590	58.97410	0.974
	PEG 10000	81.0922	-0.4983	82.44736	0.989
NaH_2PO_4	PEG 4000	72.1761	-0.3678	24.37894	0.999
	PEG 6000	67.4228	-0.3213	27.27032	0.997
	PEG 10000	79.8814	-0.4056	44.74472	0.998
K_2HPO_4	PEG 4000	65.6376	-0.4646	116.1371	0.974
	PEG 6000	72.4897	-0.5296	110.3154	0.989
	PEG 10000	128.4450	-0.7952	177.413	0.994
$(NH_4)_2SO_4$	PEG 4000	309.5294	-1.0993	11.73635	0.999
	PEG 6000	304.9436	-1.0747	10.82578	0.979
	PEG 10000	110.4330	-0.6179	119.3288	0.989

Table 2 Asparaginase and Amylase partition coefficients and recovery yeild parameters for systems based on polymer, salt and water

system	PEG	Salt	pH	ASP		Amylase	
				K_P	Y_T	K_P	Y_T
S_1	PEG 4000 (15%)	$Na_3C_6H_5O_7$. $2H_2O$ (25%)	6.8	0.08	96	0.98	92
S_2	PEG 10000 (25%)	K_2HPO_4 (16%)	6.8	0.18	88	2.66	89
S_3	PEG 6000 (26%)	$(NH_4)_2SO_4$ (15%)	6.8	0.21	86	2.54	90

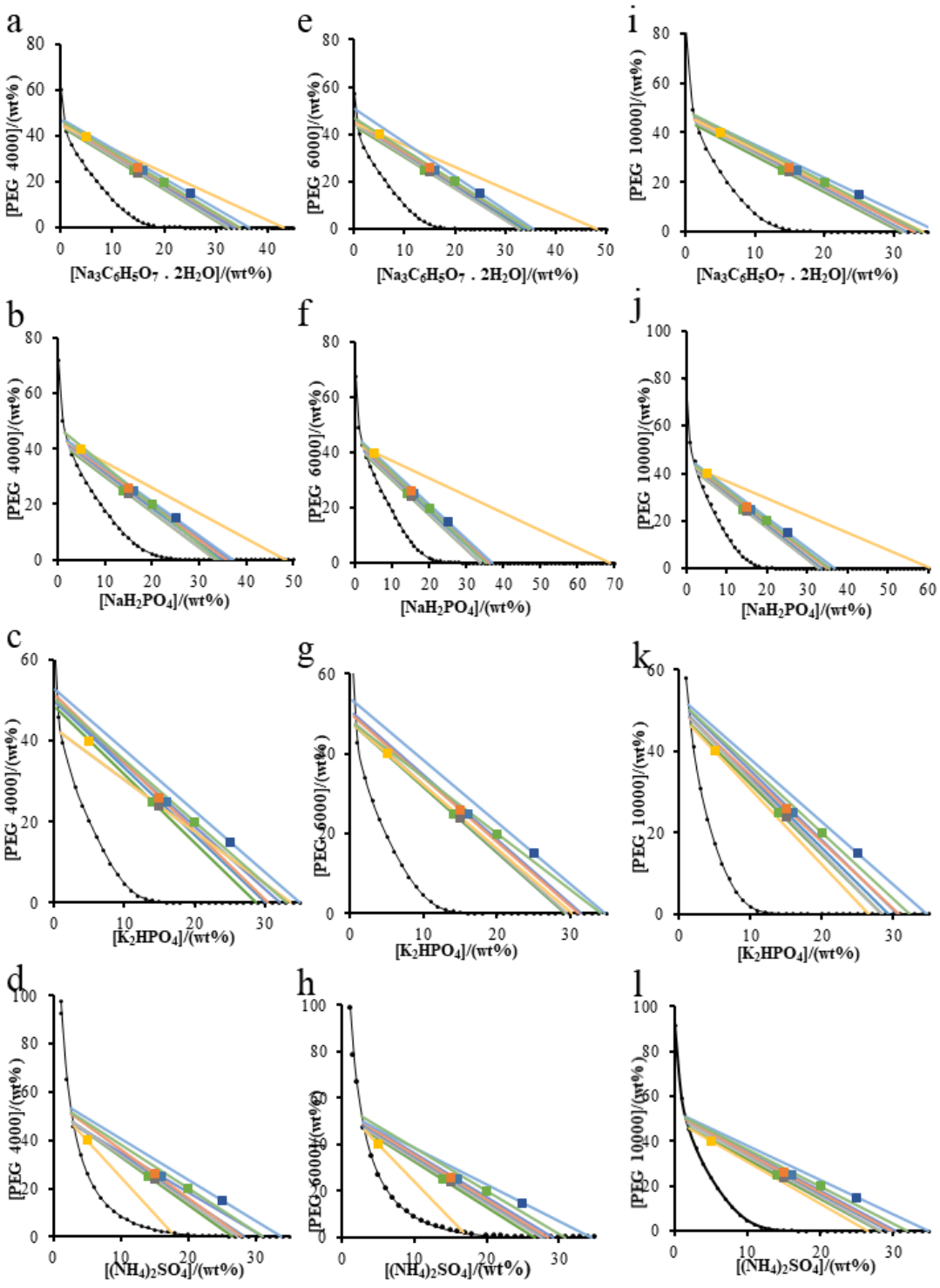

Figure 1. Phase diagrams comprising the binodal curves and respective experimental TLs for ATPSs composed of different polymers and salts.

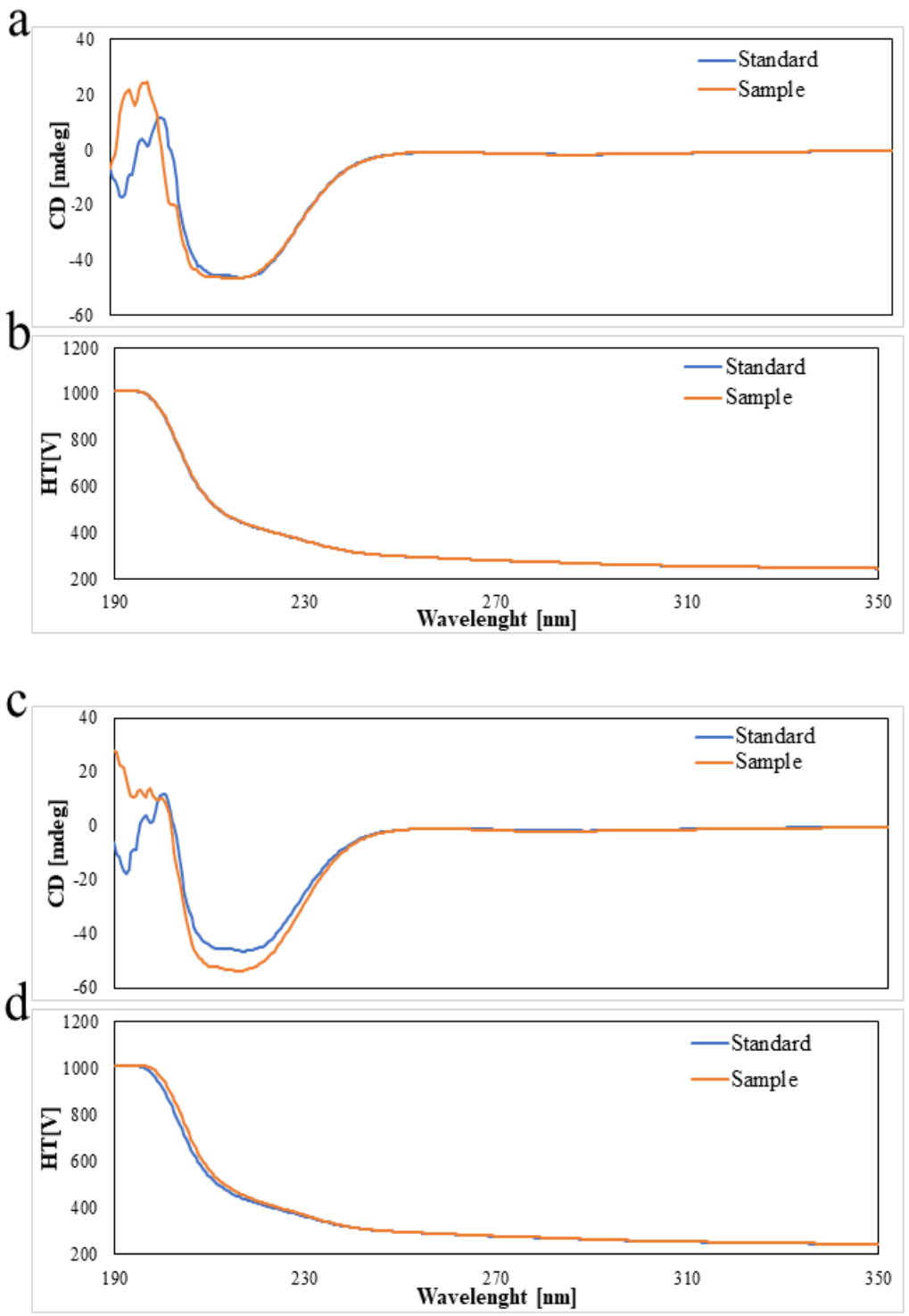

Figure 2. CD spectrum of ASP standard solution and ASP sampled from the lower phase of the optimum feed (a and b related to S_2 and c and d related to S_3).

Steady-state kinetic study compares specific activity of standard ASP and partitioned ASP in S3. Reaction time was achieved by calculating linear range of released ammonia from standard ASP and ASP of S_3. Regarding Figure 3, up to 30 minutes, the quantity of released ammonia was linear and R^2 values for standard ASP and ASP related in S3 were 0.991 and 0.990, respectively. As a result, specific activity of ASP from the bottom phase of the optimum feed (S_3) was found close to standard aqueous solution ASP (190 IU) and was around 179 IU.

ANN Model

For the selected models, the percentage of outliers using 95 % confidence bounds was found. A diagram of the ANN model is presented in Figure 4.

Figure 5 shows the R-value of dispersion of output data with respect to their corresponding target values. The high amount of R2 (0.99159) confirms an efficient model, illustrating a real relationship between the independent variables. 99 % of the variation in the response could be explained by the model. The deviation between network output and target value is more at the beginning stage of the training; however, by increasing the epochs, amounts of output and target were converged, confirming the learning relationship between input and output for the above network (Figure 6).

DISCUSSION

This article presented ATPS application to partition a biopharmaceutical, kind of ASP. The ATPS was consisted of three PEGs (Mw: 4000, 6000 and 10000) and inorganic salts ($Na_3C_6H_5O_7$. $2H_2O$, NaH_2PO_4, K_2HPO_4 and $(NH_4)_2SO_4$).

In this study, the upper phase is PEG-rich phase and the lower phase is mainly composed of salt. However, due to viscosity of PEG, some samples were formed in gel and if this point is close to the critical point, the data is omitted. In this sample, the phases were converted. Phase separation depends on the type and concentration of salt and molecular weight, weight percent, volume ratio of the phase and equilibrium characteristics of polymer in the systems. According to data, by increasing weight of PEG, separation area of the ATPS increased so lower amounts of PEGs and salts are required for phase separation, justifying

by hydrophobicity of polymer, which increases in PEGs with more Mw [26,27]. Moreover, solute such as a salt on the miscibility of an aqueous solution (salting-out effect) is a basis of phase formation in ATPS. This effect is related to the hydration strength of the salt [28-35].

The partition coefficients of proteins in ATPS are dependable on two parameters. First the PEG exclusion effect, which changes the availability of free volume for proteins in the PEG rich phase. Secondly the PEG–protein binding depends on the hydrophobic area of the protein exposed to the solvent; hence, increasing this area rises the tendency of the proteins to be in the upper (PEG rich) phase. By increasing Mw of PEG, hydrophobicity growths; consequently, hydrophobic protein moves to the upper phase (PEG rich) and finally K_{ASP} enhances [31]. Also, protein molecules were aggregated in the presence of PEG due to hydrophobic force, which is another reason of hydrophobic affinity of protein.

Charge of protein controls pH effect on K_{ASP}, which depends on pH of the solution and isoelectric point (pI) of the protein. The pH of ASP is about 9.8 [32]. In this study, effect of pH, ranging from 6.8 to 8, on K_{ASP} in the presence of PEG 10000 is more significant that of PEG 4000; accordingly, ASP concentration with negative charge increases in PEG rich phase. The relationship between polymer concentration or Mw and the free volume between polymer networks is indirect, reducing the accessible space for the biomolecules in the upper (PEG rich) phase. This phenomenon is volume exclusion effect, causes more partitioning of ASP in the lower (salt rich) phase. In contrast, resulting from salting out effect, by increasing the salt concentration in the salt rich phase, the affinity of ASP in this phase decreases, and ASP concentration increases in the PEG rich phase [33]. Also, increasing the PEG molecular weight may partition the hydrophilic enzyme to the lower (salt-rich) phase, because of increasing the hydrophobicity of PEG with the chain length [34,35].

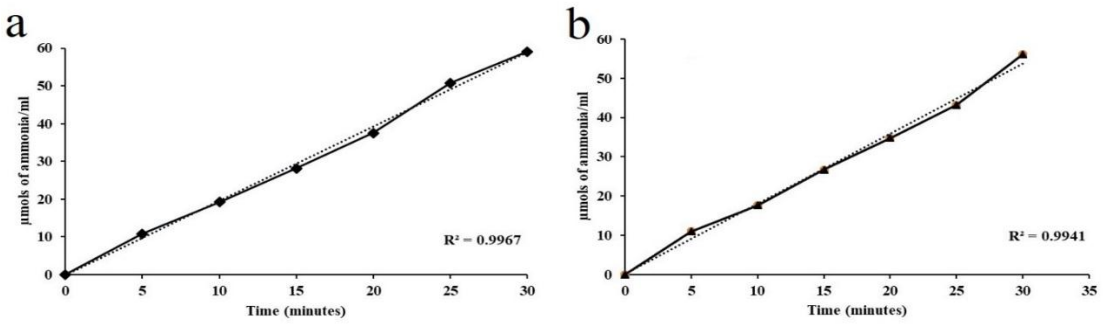

Figure 3. Bioactivity of (a) ASP standard (b) ASP sampled from the lower phase of the optimum feed related to S3.

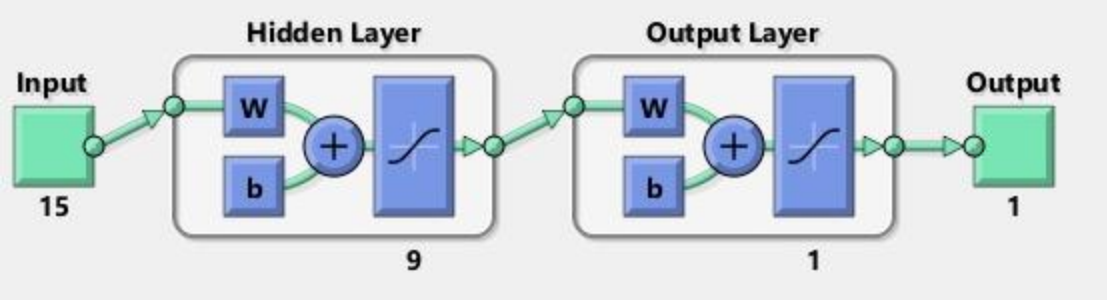

Figure 4. nntool created feed-forward neural network.

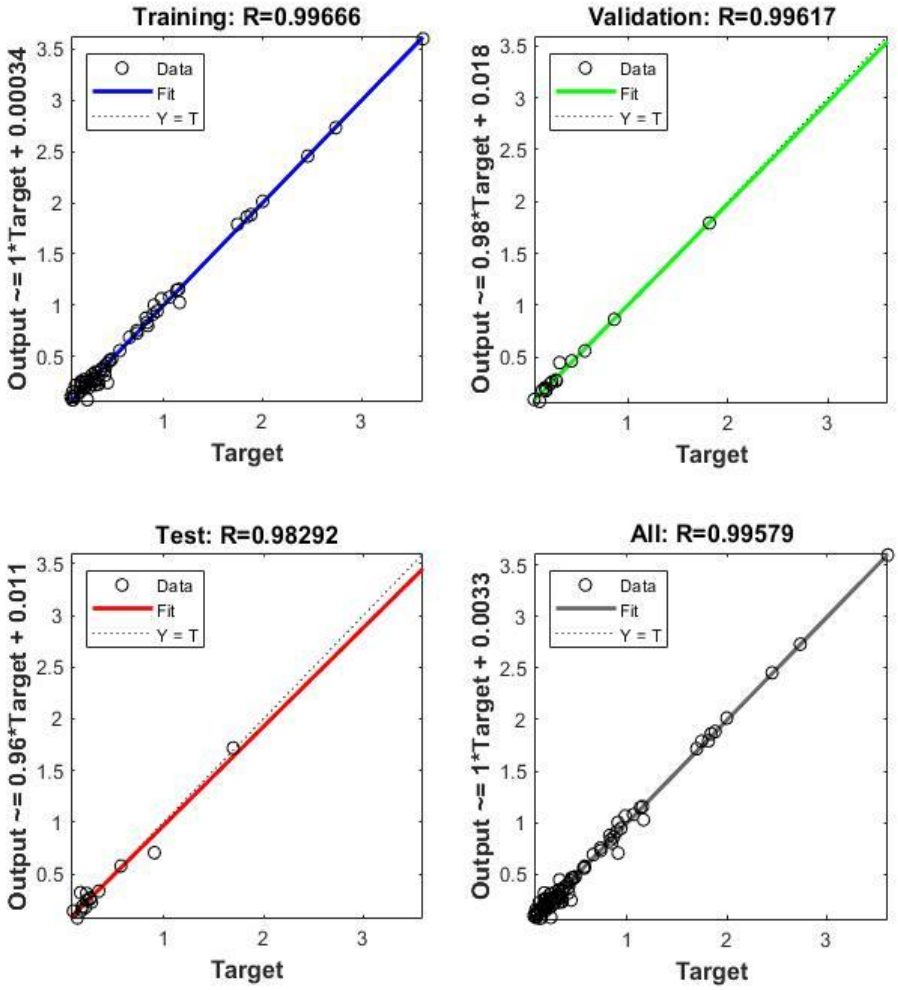

Figure 5. The linear regression between the network output values (predictive) and the target values (experimental) for $K_{ASP.}$

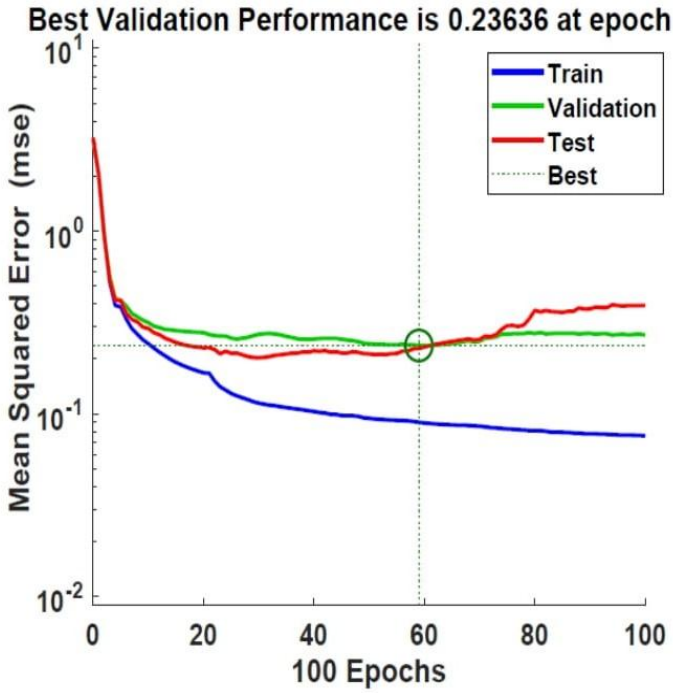

Figure 6. The convergence of the MSE with the number of iterations (epochs), during the training of the best selected feed forward network for $K_{ASP.}$

CONCLUSION

The results express that there is a common tendency for the majority of systems examined here and ASP was distributed mostly in the bottom phase (K<1). Furthermore, increasing the salt concentration have positive effect on ionic strength and enhance the protein movement to other phase (PEG rich phase) via electrostatic force so the K_{ASP} increases. K_{ASP} increases with the PEG concentration in upper (PEG rich) phase. Applicability of ATPS for separation depends on selective partition of molecules and impurities. Surface properties of proteins and phase properties effect on different phase preferences of ASP and amylase. Comparing the results indicate that in the pH of 6.8, ASP was partitioned to the lower phase, while amylase was partitioned to the upper phase. In the mentioned pH, ASP has positive charge, because its pH is about 9.8. Accordingly, the behavior of ASP separation depends on repulsion between

the charge of ASP surface and hydrogen ions at pH=6.8. CD data for S3 confirm that the structure of ASP is unaffected and remain stable. Also, the activity was followed and the relative activity was reported. The ASP partitioning was modeled by a two-layer feed-forward neural network successfully.

REFERENCES

[1]. Mehta A. Pharmaceuticals from Microbes, *Springer, New York,* 2019.

[2]. Phong WN, *et al*. Recovery of biotechnological products using aqueous two phase systems. *J. Biosci. Bioeng,* 2018. 126: 273-81.

[3]. Yang O, *et al*. Economic analysis of batch and continuous biopharmaceutical antibody production: A review. *J. Pharm. Innov,* 2020. 15: 182-200.

[4]. Barros DPC, *et al*. Predicting protein partition coefficients in aqueous two phase system. *J. Chromatogr. A.* 2016. 1470: 50-58.

[5]. McQueen L, *et al*. Ionic Liquid Aqueous Two-Phase Systems from a pharmaceutical perspective. *Front. Chem.* 2019. 7: 135.

[6]. Chen X, *et al*. Separation of recombinant monoclonal antibodies IgG201 from a cell culture supernatant using an integrated aqueous two-phase system with thermo-separating EOPO. *Sep. Purif. Technol.* 2021. 275: 119246.

[7]. Pires IS, *et al*. Selective protein purification via tangential flow filtration exploiting protein-protein complexes to enable size-based separations. *J. Membr. Sci.* 2021. 618: 118712.

[8]. Bhat M, *et al*. Affinity precipitation of monoclonal antibodies using ELP-Z in the elution without resolubilization mode. *J. Biotechnol.* 2021. 338: 1-4.

[9]. Seyedinkhorasani M, *et al*. Affinity based nano-magnetic particles for purification of recombinant proteins in form of inclusion body. *Iran Biomed J.* 2020. 24: 192-200.

[10]. Tarver CL, *et al*. Ionic liquids as protein crystallization additives. *Crystals.* 2021. 11: 1166.

[11]. Chao Y, *et al*. Emerging aqueous two-phase systems: from fundamentals of interfaces to biomedical applications. *Chem. Soc. Rev*. 2020. 49: 114-42.

[12]. Filho RFd, *et al*. Comparison of conventional and extractive fermentation using aqueous two-phase system to extract fibrinolytic proteases produced by Bacillus stearothermophilus DPUA 1729. *Prep. Biochem. Biotechnol.* 2021. 51: 191-200.

[13]. Arzideh SM, *et al*. Ion-solvent interaction of 1-decyl-3-methylimidazolium chloride and isopropanol in a quaternary aqueous two phase system for the efficient partitioning of vanillin and L-tryptophan. *J. Mol. Liq.* 2021: 332: 115860.

[14]. Ebeler M, *et al*. First comprehensive view on a magnetic separation based protein purification processes: From process development to cleaning validation of a GMP-ready magnetic separator. *Eng. Life Sci.* 2019. 19: 591-601.

[15]. Afzal B, *et al*. Separation of glatiramer acetate and its constituent amino acids using aqueous two-phase systems composed of maltodextrin and acetonitrile. *J. Ind. Eng. Chem.* 2021. 104: 544-54.

[16]. Shibata C, *et al*. Selective separation method of aggregates from IgG solution by aqueous two-phase system. *Protein Expr. Purif.* 2019: 161: 57-62.

[17]. Silva MFF, *et al*. Integrated purification of monoclonal antibodies directly from cell culture medium with aqueous two-phase systems. *Sep. Purif. Technol.* 2014. 132: 330-35.

[18]. Ferreira L, *et al*. Effect of salt additives on protein partition in polyethylene glycol–sodium sulfate aqueous two-phase systems. *Biochim Biophys Acta Proteins Proteom.* 2013. 1834: 2859-66.

[19]. Chow YH, *et al*. Characterization of bovine serum albumin partitioning behaviors in polymer-salt aqueous two-phase systems. *J. Biosci. Bioeng.* 2015. 120: 85-90.

[20]. Baghbanbashi M, *et al*. One pot silica nanoparticle modification and doxorubicin encapsulation as pH-responsive nanocarriers applying PEG/Lysine aqueous two phase system. *J. Mol. Liq.* 2022: 349: 118472.

[21]. Chen Q, *et al*. Enhancing the sensitivity of DNA and aptamer probes in the dextran/PEG aqueous two-phase system. *Anal. Chem.* 2021. 93: 8577-84.

[22]. Cowan DA, *et al*. Biocatalysts and enzyme technology. *Chem. Phys.* 2005. 206: 1448-48.

[23]. Zhang C, *et al*. A novel salt-tolerant strain Trichoderma atroviride HN082102.1 isolated from marine habitat alleviates salt stress and diminishes cucumber root rot caused by Fusarium oxysporum. *BMC Microbiology*. 2022. 22: 67.

[24]. Abedin F, S. *et al*. Mutual structural effects of unmodified and pyroglutamylated amyloid β peptides during aggregation. *J. Pept. Sci.* 2021. 27: 3312.

[25]. Dumina M, *et al*. A novel L-Asparaginase from hyperthermophilic archaeon thermococcus sibiricus: Heterologous expression and characterization for biotechnology application. *J. Mol. Sci.* 2021: 22.

[26]. Pazuki GR, *et al*. Prediction of the partition coefficients of biomolecules in polymer–polymer aqueous two-phase systems using the artificial neural network model. *Part. Sci. Technol.* 2010. 28: 67-73.

[27]. Thabit QQ, *et al*. Implementation three-step algorithm based on signed digit number system by using neural network. *J. Electr. Eng. Comput. Sci.* 2021. 24: 1832-39.

[28]. Rani A, *et al*. Changing relations between proteins and osmolytes: a choice of nature. *Phys. Chem. Chem. Phys.* 2018. 20: 20315-33.

[29]. Vicente FA, I. *et al*. Separation and purification of biomacromolecules based on microfluidics. *Green Chem.* 2020. 22:4391-4410.

[30]. Huang Y, *et al*. Phase behavior at different temperatures of an aqueous two-phase ionic liquid containing ([BPy] NO3, ammonium sulfate and sodium sulfate, water). *J. Chem. Eng. Data.* 2017. 62: 796-803.

[31]. Zolfaghar M, *et al*. Isolation and screening of extracellular anticancer enzymes from halophilic and halotolerant bacteria from different saline environments in Iran. *Mol. Biol. Rep*. 2019. 46: 3275-86.

[32]. Trimpont M Van, *et al*. Novel insights on the use of L-Asparaginase as an efficient and safe anti-cancer therapy. *Cancers (Basel)*. 2022. 14.

[33]. Gündüz U, *et al*. Optimization of bovine serum albumin partition coefficient in aqueous two-phase systems. *Bioseparation.* 2000. 9: 277-81.

[34]. Alhelli AM, *et al*. Response surface methodology modelling of an aqueous two-phase system for purification of protease from Penicillium candidum (PCA 1/TT031) under solid state fermentation and its biochemical characterization. Int. *J. Mol. Sci.* 2016. 17.

[35]. Blatkiewicz M, *et al*. Continuous laccase concentration in an aqueous two-phase system, Continuous laccase concentration in an aqueous two-phase system. *Chem. Zvesti*. 2018. 72: 555-66.